

## Numerical Simulations of the Interactions between a Vortex and a Liquid Gas Interface

J. Cousin<sup>\*</sup>, T. Menard, A. Berlemont and J. Helie<sup>†</sup>  
<sup>\*</sup> CNRS UMR 6614 – CORIA Université et INSA de Rouen  
Avenue de l'Université – BP 76801 Saint Etienne du Rouvray  
FRANCE  
<sup>†</sup> Continental Automotive SAS  
1 Avenue Paul Ourliac – BP 1149 Toulouse Cedex 1  
FRANCE

### Abstract

The present study concerns the bidimensional direct numerical simulations of the interaction between a vortex pair and a liquid-gas interface without any gravitational effects. The vortex pair is seen here as an energetic structure which is aimed to break the gas-liquid interface. By varying the vortex characteristics (size, energy,...), a series of simulations led to an energetic analysis which helps to know whether liquid flow structures such turbulent eddies are strong enough to produce small droplets during the primary breakup. All the results are re-grouped in a Reynolds-Weber numbers diagram and are discussed. The program used here computes the Navier-Stokes equation for incompressible and two-phase flows with arbitrary free surface. Interface tracking is performed with a coupled Level-Set and VOF method whereas the Ghost Fluid method is used to capture accurately sharp discontinuities.

### Introduction

In the case of pressure atomizers, internal liquid flows and sprays are produced thanks to hydraulic energy brought by mechanical systems such pumps. It is well known that these systems are rather inefficient to produce small droplets. As a matter of fact, with these atomizing systems, the initial hydraulic energy is mainly converted into spray kinetic energy and the amount of created spray surface energy is small. For instance in the case of atomizers devoted to automotive port fuel injection, Triballier *et al* [1] defined an atomization efficiency, as the ratio between the created surface energy and the brought mechanical energy, and measured efficiencies less than one per cent.

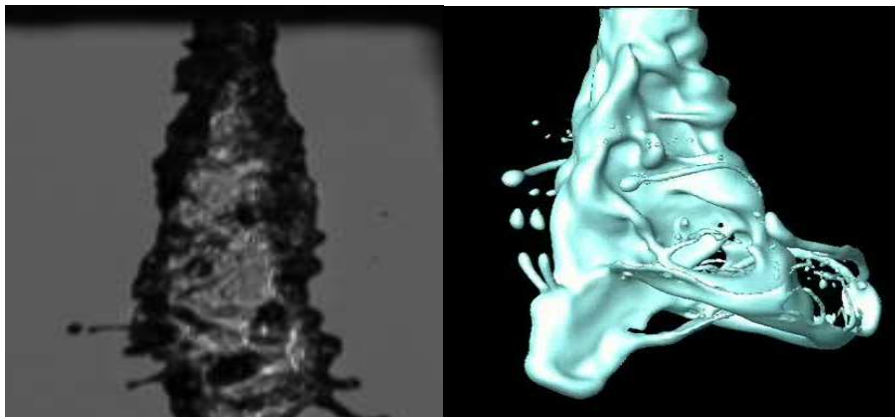


**Figure 1.** Example of a ligament formation (visualized (left) and calculated (right) of a water jet issuing from a triple disk injector [2])

In the case of jets discharged from pressure atomizers into still gases, Faeth *et al* [3] explain that the ejection of droplets along the primary breakup process is due to liquid turbulence. Authors argue also that the aerodynamic effects remain negligible in the case of large liquid/gas density ratios. In addition, based on experimental data they found correlations between the size of the ejected droplet and a Weber number based on the radial integral scale. All these considerations invite us to better describe the drop formation generated from energetic

<sup>\*</sup> Corresponding author: cousin@coria.fr

vortical structures. Figure 1 is an illustration of droplet formation issued from such a structure. The present study is intended to simulate the formation of drops resulting from the presence of a vortical structure inside the liquid.

In the literature, many studies can be found about the interaction between a vortex and an interface. For instance Kadowaki and Hasegawa [4] reviewed the studies concerning the interaction between a flame and a vortical structure. They showed that the interface behavior is mainly controlled by the ratio between the maximum circumferential vortex velocity and the flame speed. Other studies can be found in this research field but also in the case of a solid interface (Archer *et al* [5]) or deformable interfaces subjected to gravity effects as studied by Yu and Tryggvason [6]. In the latter case, authors were more concerned by the effects of the Froude number whereas the surface tension effects were ignored with a Weber number set to infinite. The present study is devoted to analyze the deformation of a liquid-gas interface subjected to the presence of a vortex including surface tension effects. First, the numerical method is briefly detailed as well as the description of the problem. Second, numerical results are presented and discussed. Finally all the simulated cases are reported into a Reynolds-Weber number diagram that allows separating cases where vortex is strong enough to lead to a liquid detachment.

### Numerical Method

A numerical code (newly called ARCHER) has been developed to describe the dynamic of liquid/gas interfaces. The Level Set method is used to capture the interface motion. Resolution of Level Set transport equation is coupled with the resolution of incompressible Navier-Stokes equation and Ghost Fluid method [3, 7] is applied to take into account jump conditions at the liquid/gas interface. This approach was successfully applied on droplet collisions [8], Rayleigh jet atomization [9] and droplet evaporation [10].

The Level Set method suffers from mass loss which becomes problematic in situations with strong stretching near the interface. We so develop the CLSVOF method introduced by Sussman and Puckett [11]. This method couples Level Set and Volume Of Fluid approaches. Information given by volume fraction enforces the mass conservation and the Level Set function ensures accurate topological information. In addition an MPI parallelization was implemented and applied on high speed liquid jet [9].

The version used in this study is in 2D configuration. The resolution of equation is performed on uniform staggered grids with finite difference discretizations. Spatial differencing for convective terms is achieved with a WENO5 scheme and an Adams-Bashforth scheme is used for temporal derivatives. Poisson equation discretization, with second order central scheme, leads to a linear system solved by a multigrid algorithm for preconditioning a conjugate gradient method.

### Description of the problem

The present study investigates the temporal evolution of a vortex pair located inside the liquid phase. The vortex pair is built in order to move toward the liquid gas interface. Therefore the energy brought by the vortical structure deforms the interface. In this work, we numerically controlled the vortex pair by using the Oseen's vortex. The mathematical form of such vortices expresses the tangential velocity as a function of the distance from the vortex center ( $r$ ):

$$u_{\theta} = 1.56697 u_{\theta_{max}} \left( \frac{l}{r} \right) \left[ 1 - \exp\left( -\frac{r^2}{l^2} \right) \right] \quad (1)$$

where  $u_{\theta_{max}}$  is the maximum velocity encountered inside the vortex and  $l$  is a vortex characteristic length. The constant in the equation (1) is derived from the original expression of the Oseen's vortex where the velocity profile was expressed as a function of the circulation.

Figure 2 illustrates the chosen 2D configuration at the initial time;  $d$  and  $L$  represent the distance between the two vortices and the initial distance from the interface respectively.  $X$  and  $Y$  are the dimensions of the computational domain. In the present analysis these four geometrical parameters are kept constant and proportional to the vortex characteristic length, i.e.:

$$d = 2l; L = 15l; X = 60l; Y = 30l \quad (2)$$

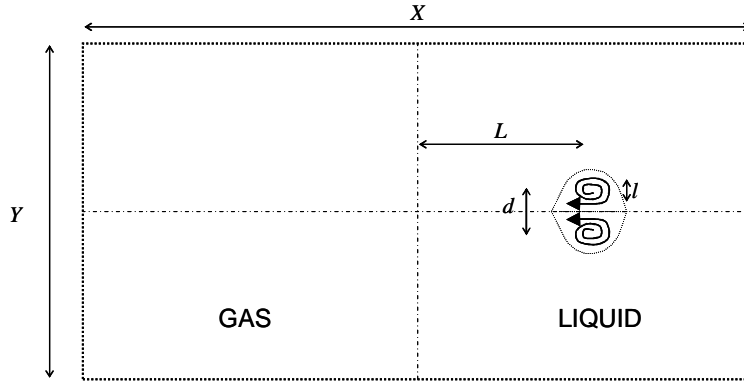


**Figure 2.** Configuration of the problem

The computational domain is meshed with a regular cartesian grid ( $NX$  and  $NY$  cells in horizontal and vertical directions respectively) and is constituted of two separated fluids. When the simulation starts, the liquid ( $\mu_L$  and  $\rho_L$  are the dynamic viscosity and density respectively) fills the half right of the computational domain and the left part is filled with gas ( $\mu_G$  and  $\rho_G$  are the dynamic viscosity and density respectively). At the initial computational time, the gas-liquid interface which is characterized by the surface tension coefficient  $\sigma$  is unperturbed and vertical whereas the vortex pair is injected within the liquid at the distance  $L$  from the interface.

The studied physical phenomenon depends on six numbers without dimension: two are length ratios, the liquid-gas density and the viscosity ratios as well as Reynolds and Weber numbers; they are defined as follows:

$$Re = \frac{\rho_L u_{\theta max} l}{\mu_L}, \quad We = \frac{\rho_L u_{\theta max}^2 l}{\sigma}, \quad R = \frac{\rho_G}{\rho_L}, \quad M = \frac{\mu_G}{\mu_L}, \quad \frac{d}{l} \text{ and } \frac{L}{l} \quad (3)$$

In the present investigation, the two last numbers are kept constant and equal to 2 and 15 respectively. It can be remarked that the  $L/l$  is a parameter that can be removed if one considers the vortex/interface interaction only. In other words, after the vortex solution is numerically established, it exists only one solution for a given  $Re$  and  $L/l$  before the interaction with the interface. However we choose here to keep it, because this ratio and the Reynolds number return an information about the effect on the initial vorticity location. This information is of real interest for atomization process. For instance, with liquid jets, the effects of the vorticity location have to be understood since coherent structures or intense shear zones emerge from the discharge orifice. A second remark concerns the parameter  $d/l$  which characterizes the vortex pair family about its internal structure. This parameter affects the vortex self velocity and may affect the dynamic of the ligament shape. It has also to be kept in mind that the initiated vortices are not solution of the Navier Stokes equations. However after this initialization the two vortex cores evolve freely with time.

### Results and Discussion

Figure 3 illustrates the temporal evolution of a water-air interface subjected to the presence of a pair of vortices. Due to the initial flow field inside the liquid phase, a pair of vortices moves towards the interface whereas a less energetic pair of vortices moves on the opposite direction. This behavior is due to the momentum conservation of the liquid. As time increases, the vortex which moves towards the interface loses a part of its initial kinetic energy due to liquid viscosity and reaches the interface. The interface is then perturbed with a characteristic length close to the vortex length scale. In the illustrated situation, the remaining kinetic energy is sufficient to create a ligament whose length is large enough to promote a Rayleigh-type breakup; a droplet is then formed. In this case, the calculation reports that the vortex pair has enough energy to produce a droplet. It can be observed that a large amount of energy was consumed in the surface creation. Therefore the droplet has a negligible kinetic energy and stays at a fixed location.

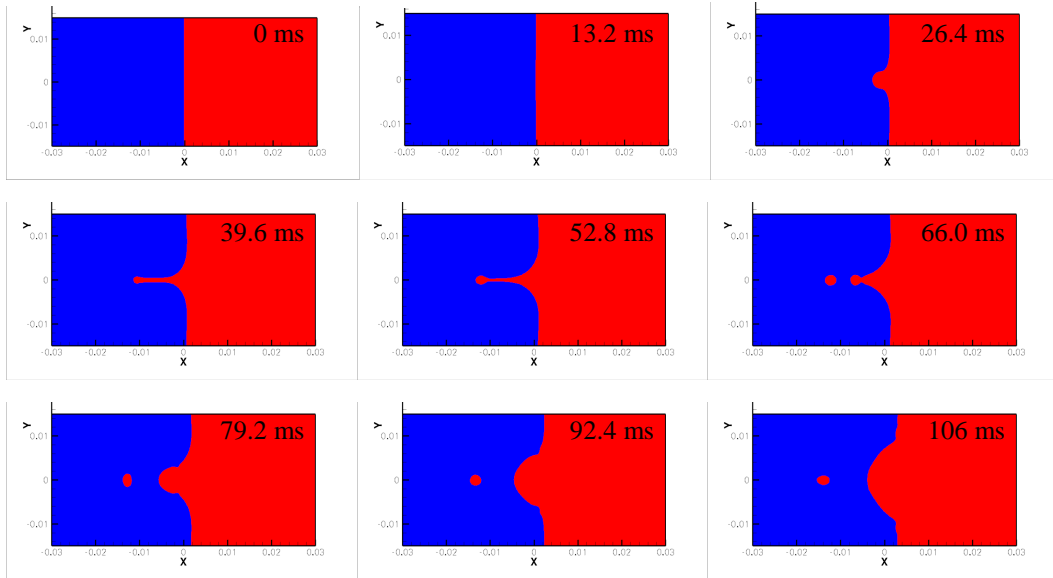


**Figure 3.** Temporal evolution of the liquid gas interface

$$(Re = 880, We = 13.89, R = 1.126 \cdot 10^{-3}, M = 1.566 \cdot 10^{-2})$$

Figure 4 shows the temporal evolution of both kinetic and surface energies for the investigated case illustrated in Fig. 3. The kinetic energy per unit of length ( $E_c$ ) is calculated on the whole computational domain including both liquid and gaseous phases and the surface energy per unit of length ( $E_s$ ) is defined as the product of the surface coefficient  $\sigma$  (set to  $72 \cdot 10^{-3} \text{ Nm}^{-1}$  here) by the calculated length of the interface. During the approach of the vortex towards the interface, obviously the surface energy does not vary whereas a decrease of the kinetic energy is observed. This decrease is due to the natural viscous dissipation. When the vortex starts to deform the interface, a sharp decrease of the kinetic energy is accompanied with an increase of the surface energy leading to a rather constant sum of both energies during the formation of the droplet. This result tends to show that a conservation of both energies is achieved during the breakup process.

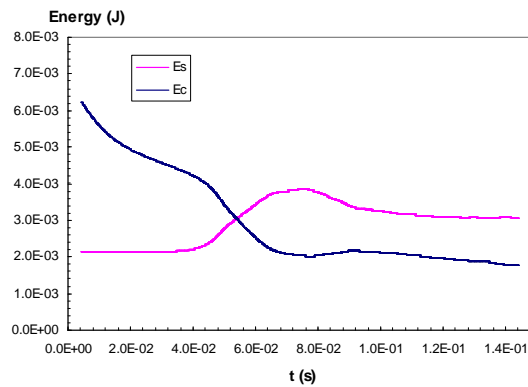


**Figure 4.** Temporal evolution of the kinetic ( $E_c$ ) and surface ( $E_s$ ) energies ( $Re = 880, We = 13.89,$

$$R = 1.126 \cdot 10^{-3}, M = 1.566 \cdot 10^{-2})$$

The effect of the mesh size is also investigated. For the same case as described above, Figure 5 shows the temporal evolution of both energies for two meshes. It can be observed that the more refined mesh leads to less dissipation before the vortex reaches the interface. However, it can be observed that the temporal variations of both energies weakly depend on the mesh size. In addition, for the investigated case, the use of both meshes leads to the production of a single droplet. Therefore as far as the present study is concerned and regarding the large number of physical investigated configurations, the mesh size  $NX \cdot NY = 256 \cdot 128$  will be considered only.

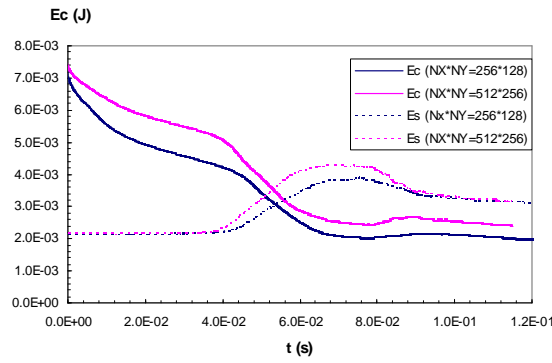


**Figure 5.** Temporal evolution of  $E_c$  and  $E_s$  – Effect of the mesh size ( $Re = 880$ ,  $We = 13.89$ ,  $R = 1.126 \cdot 10^{-3}$ ,  $M = 1.566 \cdot 10^{-2}$ )

In the present investigation, it has been also verified that the calculations respect the properties of similitude evoked earlier. The left side of Fig. 6 shows the temporal evolution of the kinetic energy for four different investigated cases. These cases are all characterized by the same  $Re$ ,  $We$ ,  $R$ ,  $M$ . When the kinetic energy is plotted under a dimensioned form, it can be clearly observed that the temporal evolution depends on the parameters which were varied in these four calculations ( $u_{\theta max}$ ,  $\sigma$  and  $l$ ). In parallel the right side of Fig.6 clearly shows that when kinetic energy is divided by its initial energy and by using a reduced time  $t^*$  defined by :

$$t^* = \frac{u_{\theta max} t}{l} \tag{4}$$

all curves fit in a single one. A similar behavior is observed when the surface energy is considered as well as the morphology of the interface as a function of reduced time. These results validate the good behavior of the numerical code to simulate such a process.

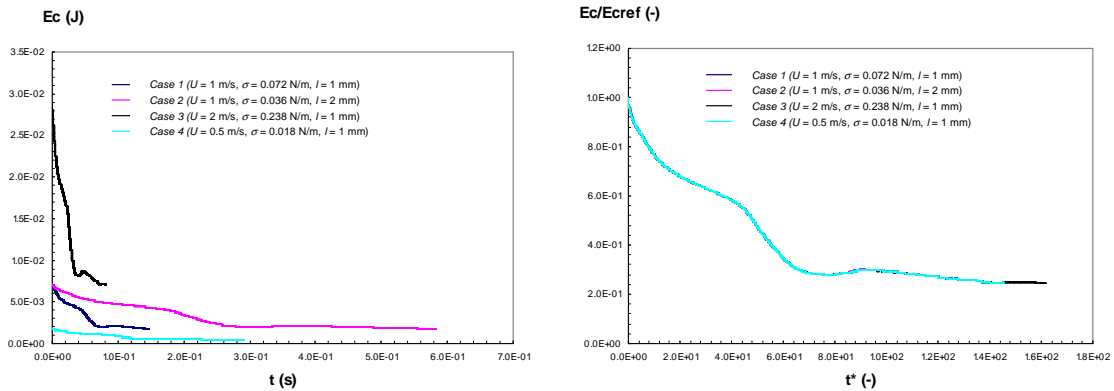


**Figure 6.** Temporal evolution of the kinetic energy and reduced kinetic energy (right) ( $Re = 880$ ,  $We = 13.89$ ,  $R = 1.126 \cdot 10^{-3}$ ,  $M = 1.566 \cdot 10^{-2}$ )

A series of simulations were performed in order to achieve a parametric study to find out the conditions that allow the production of at least one droplet for a given initial vortex. In this investigation, all the calculations were performed with the mesh size  $NX*NY = 256*128$  in order to get fast and rather accurate results. For this parametric study, all quantities without dimension were kept constant except both Reynolds and Weber number. Figure 7 summarizes the interface behavior in a  $Re-We$  diagram. Each symbol represents a single calculation and the line represents the limit between the two possible behaviors that is to say a deformation with or without a droplet detachment.

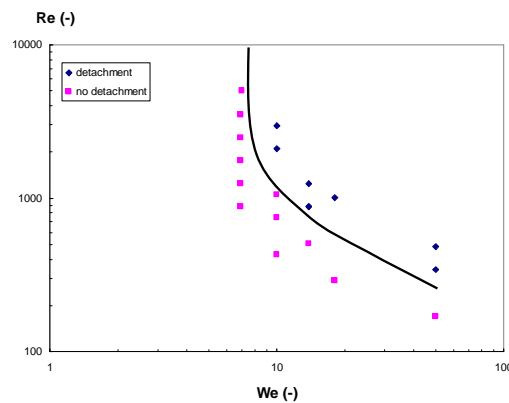


**Figure 7.** Temporal ( $Re = 880$ ,  $We = 13.89$ ,  $R = 1.126 \cdot 10^{-3}$ ,  $M = 1.566 \cdot 10^{-2}$ )

As it can be seen on this diagram, for a given Weber number, the Reynolds number needs to be higher than a critical value to ensure a drop formation. In addition, the lower the Weber number, the higher the critical Reynolds number. Regarding the investigated range of Weber numbers, for  $We$  higher than 20, the limit that allows the interface to break shows a linear behavior in the log-log  $Re-We$  diagram. The results show either that a lower limit exists in terms of Weber number; above this critical value of Weber number, any values of Reynolds does not allow the interface breakup.

## Conclusion

In the present study, the interaction between a vortex and a liquid-gas interface was investigated. The investigated configuration was 2D and the vortical structure was initiated with the analytical Oseen's vortex. The results were organized through a dimensional analysis and we demonstrated that the investigated configuration is described with six numbers without dimensions; two of them are linked with the liquid turbulence generation only. Among these numbers, ratios of densities and viscosities were kept constant whereas the Weber and Reynolds numbers were varied. We showed that a combination of the values of these last both numbers may lead to a strong interface deformation including a drop formation. For the investigated situations, the Weber number needs to be higher than a critical value, estimated to about 7, is needed to allow the production of one drop. In addition by reporting all the numerical results, in a Reynolds-Weber number diagram, we showed that for a given Weber number higher than a critical value, a minimum Reynolds number is needed to detach a droplet. These results are of paramount importance in order to know whether a given vortical structure as the ones present in turbulent liquid jets is strong enough to produce droplets.

## References

- [1] Triballier, K., Cousin, J., Dumouchel, C., *ILASS Europe*, Zaragoza, Spain, September 2002.
- [2] Berlemont, A., Cousin, J., Ménard, T., Grout, S., *ASME*, Montréal, Canada, August 2010.
- [3] Faeth, G.M., Hsiang, L.P., Wu, P.K., *Int. J. Multiphase Flow* 21:99-127 (1995).
- [4] Kadowaki, S., Hasegawa, T., *Progress in Energy and Combustion Science* 31:193-241 (2005).
- [5] Archer, P.J., Thomas, T.G., Coleman G.N., *J. Fluid Mech.* 642:79-94, (2009).
- [6] Yu, D., and Tryggvason, G., *J. Fluid Mech.* 218:547-572, (1990).
- [7] Fedkiw, R. Aslam, T., Merriman, B., Osher, S., *J. Comput. Phys.* 152:457-492, (1999).
- [8] Tanguy, S., Berlemont, A., *Int. J. Multiphase Flow* 31:1015-1035 (2005).
- [9] Menard, T., Tanguy, S., Berlemont, A., *Int. J. Multiphase Flow* 33:510-524 (2007).
- [10] Tanguy, S., Menard, T., Berlemont, A., *J. Comput. Phys.* 221:837-853, (2007).
- [11] Sussman, M., Puckett, E.G., *J. Comput. Phys.* 162:301-337, (2000).